A Control Strategy for a Multi-Terminal HVDC Network Integrating Wind Farms to the AC Grid

Mohammad Khenar[a], Jafar Adabi[a], Edris Pouresmaeil[b,c], Asghar Gholamian[a], and João P. S. Catalão[b,c,d]

[a] *Faculty of Electrical and Computer Engineering, Babol (Noshirvani) University of Technology, PO Box 484, Babol, Iran*
[b] *INESC-ID, Instituto Superior Técnico, University of Lisbon, Av. Rovisco Pais, 1, 1049-001 Lisbon, Portugal*
[c] *C-MAST, University of Beira Interior, R. Fonte do Lameiro, 6201-001 Covilhã, Portugal*
[d] *INESC TEC and Faculty of Engineering of the University of Porto, R. Dr. Roberto Frias, 4200-465 Porto, Portugal*

Abstract:

This paper describes a novel control strategy of voltage source converters (VSC) in large-scale wind farm applications, in order to achieve a constant DC voltage for connecting to the long transmission system based on multi-terminal high voltage direct current (HVDC) technology. The control strategy is based on a multi-loop current and voltage control for tracking the predetermined value of the DC link voltage in the rectifier side station to achieve proper performance in the irregular circumstances of wind farm operation. In addition, the control strategy is able to transmit the maximum input power to the consumption side in different situations in grid side converter. Grid connection of the HVDC system is analysed under two conditions: balanced AC grid, and connection of unbalanced nonlinear load into the AC grid. The control strategy guarantees injection of minimum harmonic current components from the grid to the loads. MATLAB simulation results are presented to demonstrate the effectiveness of the proposed strategy for different types of variations in AC voltage amplitude and frequency of wind turbines output voltage.

***Index Terms*-Wind farms; high voltage direct current (HVDC); power quality; voltage source converters (VSCs).**

I. Introduction

Energy consumption is ever increasing and over the past decades, the increment in energy demand has been highly balanced by capacity development of conventional power sources. But, a further electricity generation to balance energy consumption is considered by unsustainable energy sources, especially due to limited source of their primary energies and due to negative impacts they introduce into the environment. In order to supply the future electricity demand as well as to replace ageing existing generations, a number of new generation technologies based on the renewable energy sources e.g. Wind and solar have been developed. In European countries, development to wind power plants is growing fast for electricity generation; but still a small percentage of the energy demand is supplied by contribution of wind power sources[1, 2].

* Corresponding author at INESC TEC and Faculty of Engineering of the University of Porto, R. Dr. Roberto Frias, 4200-465 Porto, Portugal.
E-mail address: catalao@ubi.pt (J.P.S. Catalão).

With the purpose of integrating the future far offshore wind farm power plants in to the power grid and, regarding the capacity of these plants, long transmission lines with higher capacity would be essential[3]. But, variable wind speeds and linked generated power would result in a low capacity factor of the transmission and consequently relatively high transmission cost per amount of energy delivered. This capacity factor will be increased by connection of multi offshore wind power plants into the transmission lines[4].Furthermore, if the transmission is extended more, it can be used to smooth power trading between different societies as well as evacuate power from the wind power plant[5]. If we consider these solutions, multiple offshore wind farms would be integrated to multiple onshore power grids and consequently it would lead to the development of a transnational offshore network [6-8].

High-voltage direct-current transmission (HVDC) technology can be considered as a suitable alternative for such a multi-terminal offshore network, where huge amount of power can be transmitted over a long distance[9-11]. Furthermore, because the offshore network can act as a power pool where power can be injected to and extracted from the network at different nodes, control of direction of power during maintaining voltage in the network is needed. Implementation of voltage source converter HVDC (VSC-HVDC) technology is a constructive solution for changing the direction of power while maintaining voltage in the DC network [12, 13].In addition, an independent control for active and reactive power can be performed.

A number of control strategies have been proposed in the literature for operation of a multi-terminal VSC-HVDC network, e.g., Combined and coordinated control [14, 15], current margin control[5, 12, 13, 16], voltage margin control [17], and AC-side voltage control [17-19]. Current margin control is a standard method for point-to-point line commutated converter (LCC) based HVDC systems in which LCC terminals work in one of constant current, constant firing angle and constant turn-off angle control methods. Voltage margin control is a common control strategy in VSC based HVDC system, which is dual of mentioned current margin control. Terminals can change the power range in order to regulated DC side voltage according to the defined margins which is determined by central controller. AC-side voltage control is generally used for point-to-point HVDC systems with standalone loads such as offshore oil platforms or supplying of small islands. Grid side terminal is responsible for AC voltage regulation while other terminals are responsible for DC voltage regulation. To achieve constant AC voltage at grid side, DC side current has to be controlled. Combined and coordinated control is a type of current margin control in which inverter works in constant turn-off angle mode to regulate DC voltage and rectifier controls DC side current using voltage errors and by combination and coordination of voltage and current.

Each presented method has its own advantages and disadvantages. For instance, [20] presented a precise control technique but it makes the control implementation more complex by increasing the system calculations. Therefore, a powerful processor is required in order to control network operation with a fast response for closed loop calculations of its instantaneous conditions at different units. Control coordination between sending and receiving units of the power is another worth mentioning issues, which needs to be considered in multi-terminal networks [21]. This necessitates a radio communication

coordinator between rectifier and inverter units in such systems in order to keep maximum controllable power transfer during variations at both generation and consumption sides. Consequently, it adds to the complexity of the control system.

This paper presents a control strategy for a MTHVDC system in which each rectifier and inverter units has its own control task in order to avoid complexity of the control system. This means an independent operation of sending and receiving of the power, which eliminates telecommunications coordinators. A regulatory system has been proposed to guarantee the generation of safe and stable DC voltage in the rectifier side of HVDC transmission lines during different operating conditions of wind turbines. Managing active and reactive powers at their desired values is carried out by controlling of an interfaced voltage source inverter to the power grid.

The rest of the paper is organized into three sections. Following the introduction, the general schematic diagram of a multi-terminal DC system with three terminals as a case study, and control of wind farm side and grid side converters under different conditions will be introduced in section II. Moreover, simulation results have been performed to demonstrate the efficiency and applicability of the developed control strategy in Section III. Finally, conclusions are drawn in Section IV.

2. MTDC Structure and control of converters

Figure 1 shows the block diagram of a three terminal MTDC system based on VSC converters, which are connected to an AC grid. This system includes two wind farm terminals and a terminal connected to the grid. Since the variable wind power is the input driving force of turbines, the output voltage of wind turbines is in the form of unregulated AC with variations in both amplitude and frequency.

A control system must have the capability to regulate the output voltage in a predetermined reference during mentioned variations (by controlling AC to DC converter). As the terminals in MTDC structure are located in different places and they use various amount of wind energy, the control system should help each terminal to deliver constant DC voltage regardless of their unstable and different AC input voltage. Then, this voltage would be converted from DC to AC in the grid side inverter to produce regular and stable AC voltage.

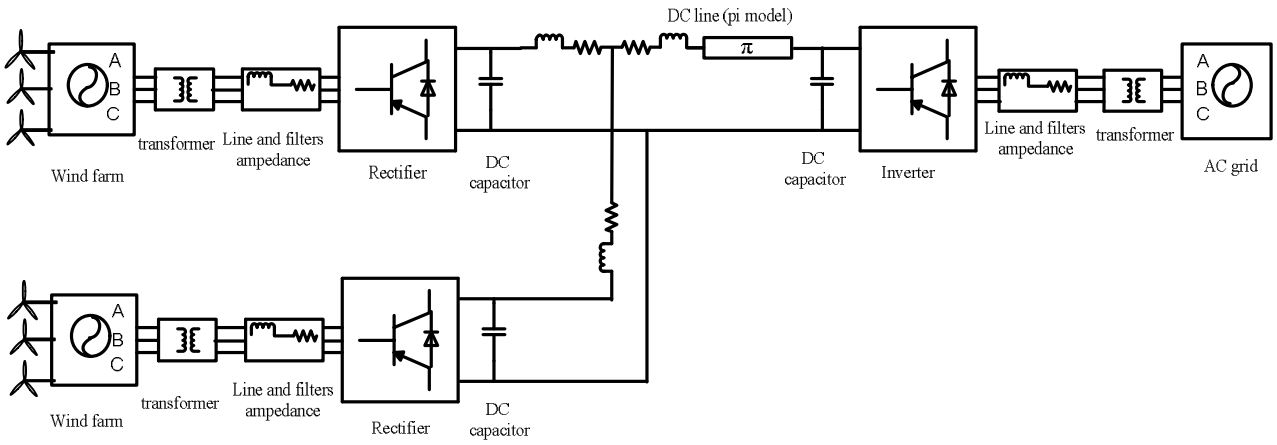

Figure 1. Three terminal MTDC model.

2.1. Control of wind farms side converter to regulate DC link voltage

As shown in Fig.2, the principle of this control method is based on a chain of control loops. Each inner loop includes a series of reference values, which are specified by the designer or other loops. The output production of the outer control loop is the reference voltage to generate the switching pattern for the power electronic converters.

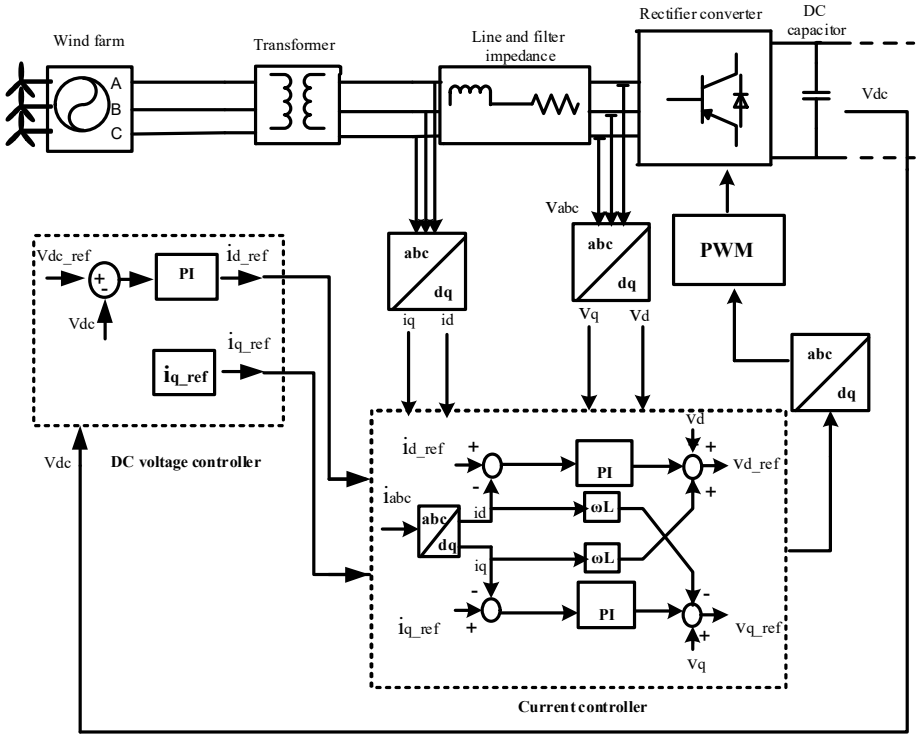

Figure 2. Diagram of wind farm side controller loops in order to regulate DC link.

As shown in inset figure of Fig.2 (DC voltage regulator), DC link capacitor is compared with its reference value and then regulated via PI controller to generate reference value of i_d. This current obtains the inputs for the current controller to generate reference voltages for the converter.

From Fig .2 and neglecting resistance of line impedance, AC voltage of the converter can be calculated as:

$$v = L\frac{di}{dt} + u \tag{1}$$

Rewriting (1) in the Laplace domain leads to:

$$V(s) = sLI(s)+U(s) \tag{2}$$

where V is the voltage at the common bus, L is the leakage inductance of the phase reactor, I is the current flowing at the ac side of the converter, U is the voltage generated by the converter and s is the Laplace operator.

Transforming (2) to the dq components results in:

$$v_d = sLi_d - \omega Li_q + u_d \tag{3}$$

$$v_q = sLi_q + \omega Li_d + u_q \tag{4}$$

ωLi_q and ωLi_dleads to a cross coupling between d and q axis quantities which makes the independent control of active power more complex. In other words, when $i_q$is regulated to control the reactive power, $v_d$will be altered, and thus, the active power will also change. In order to eliminate the cross coupling, $v_d$and $\omega \mathrm{Li_q}$ are fed forward on the *d*-axis controller while $v_q$and $\omega \mathrm{Li_d}$are fed forward on the *q*-axis controller.

The voltage reference values are then transformed to the *abc* quantities and v_{d-ref} and v_{q-ref} are fed as inputs to the controlled voltage source.

2.2. Control of the MTDC converter in the consumption side

After generation of regulated DC voltage in unstable circumstances of wind farms. It is time to deliver this voltage to the AC grid. At first, the control method should be able to transmit the maximum input active power to the grid in different conditions. Also, it should inject the least the amount of the current harmonics in to the consumers and grid. In order to be able to control the active and reactive power independently, the control scheme implemented on the grid side voltage source converter is developed based on the vector control method. The active and reactive power exchanged at the common bus can be calculated as:

$$P = v_a i_a + v_b i_b + v_c i_c \tag{5}$$

$$Q = \frac{1}{\sqrt{3}}(v_{ab} i_c + v_{bc} i_a + v_{ca} i_b) \tag{6}$$

v_a,v_b,$v_c$are three phase voltage at the common bus and i_a ,i_b,i_c are three phase currents flowing at the ac side of the converter. Transforming (5) and (6) to the *dq0*components and writing the results in pu of the converter rated capacity leads to:

$$P = v_d i_d + v_q i_q + 2v_0 i_0 \tag{7}$$

$$Q = v_q i_d - v_d i_q \tag{8}$$

2.2.1. Connection to the stable grid

For a balanced three phase system, the *0* components are equal to zero. Moreover, by considering $v_d$aligned in phase with v_d,$v_q$is zero. Therefore, (7) and (8) can be rewritten as:

$$P = v_d i_d \tag{9}$$

$$Q = -v_d i_q \tag{10}$$

It can be seen that the active power and the reactive power are now decoupled. In other words, the active and reactive powers can be controlled independent of each other by regulatingi_d and i_q respectively.

This control strategy is based on a current control method and SRF transformation. The grid frequency should be sampled by the PLL block. Three-phase grid currents should be transformed from abc to dq in this frequency according to the equation (11). Then, these currents are compared with their references (which can be calculated from power references from (9) and

(10)). The error values are regulated through PI controllers and then, transformed to the abc frame in order to produce voltage references for PWM block. Schematic diagram of this control is depicted in Fig.3.

$$\begin{bmatrix} i_d \\ i_q \\ i_0 \end{bmatrix} = \sqrt{\frac{2}{3}} \begin{bmatrix} \cos(\theta) & \cos(\theta - \frac{2\pi}{3}) & \cos(\theta + \frac{2\pi}{3}) \\ \sin(\theta) & \sin(\theta - \frac{2\pi}{3}) & \sin(\theta + \frac{2\pi}{3}) \\ \frac{1}{\sqrt{2}} & \frac{1}{\sqrt{2}} & \frac{1}{\sqrt{2}} \end{bmatrix} \begin{bmatrix} i_a \\ i_b \\ i_c \end{bmatrix} \quad (11)$$

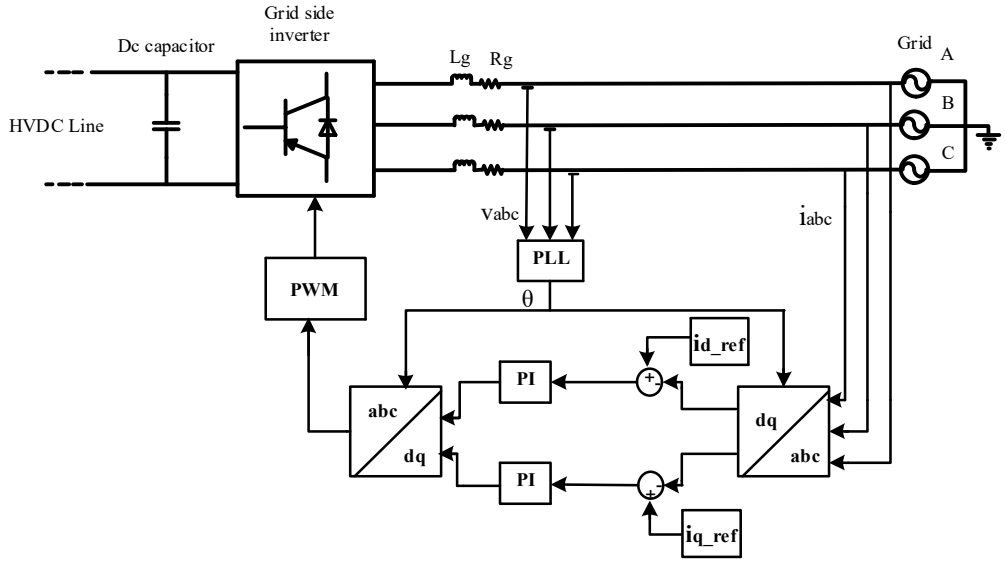

Figure 3. Schematic Diagram of grid side control in Connection to the stable grid.

2.2.2. Connection to AC grid and an unbalanced nonlinear load

Nowadays, nonlinear loads are widely spread in a power network from a wide range of high power industrial devices to very low power household appliances. These loads may pollute the network with high amounts of harmonics and draws reactive power from network. Figure4 shows a MTDC system connected to the AC grid in which an unbalanced nonlinear load is connected to the to the point of common coupling (PCC).

This unbalanced nonlinear load may cause instability in the grid side current by producing an unbalance nonlinear current. After connection of MTDC to PCC, it can supply the grid and load powers as well as improving the power quality. It means that, in addition to perform as an independent DG, it also acts as an active power filter (APF) to improve the power factor and THD. In this particular case, the control method should work as the following way to comply the required performance of MTDC system. According to Fig .4, harmonic injection and active power injection blocks are used to prepare required current references for power converter. A hysteresis band current control (HBCC) is used to obtain switching pulses of the converter.

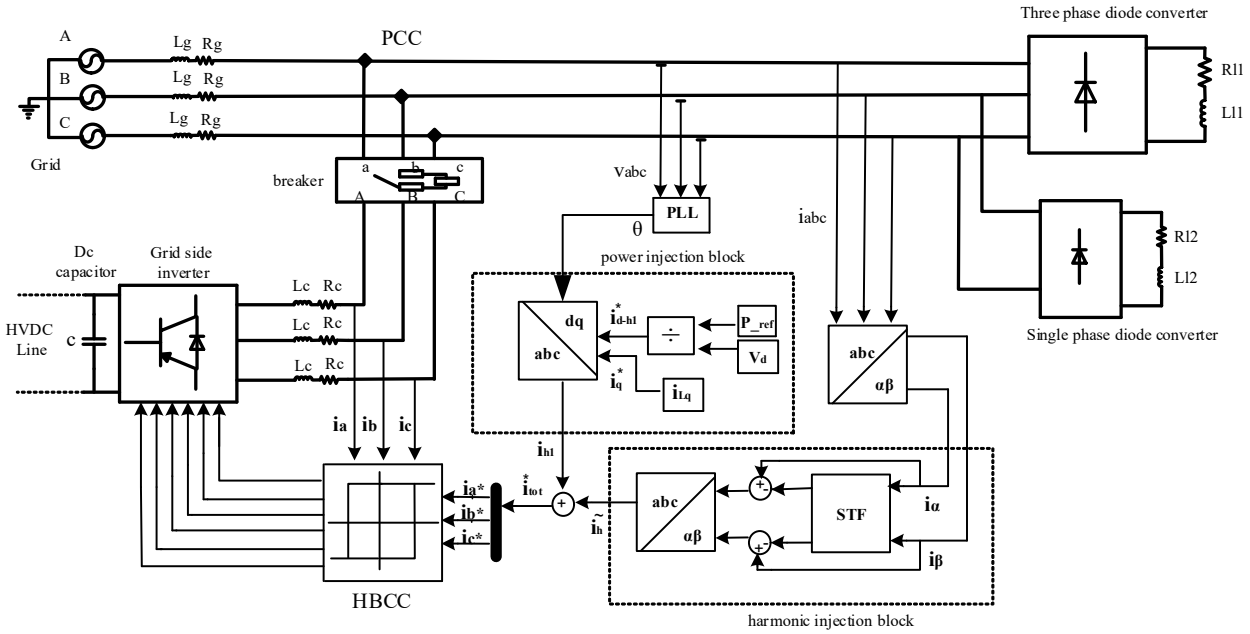

Figure 4. Schematic Diagram of grid side control in Connection to the PCC between the AC grid and unbalanced nonlinear load.

According to (9) and (10), It can be concluded that current reference of grid side converter has to be considered as q-component of load current in order to compensate load reactive power. Therefore, we have:

$$i_q^* = i_{lq} \tag{13}$$

Active power transfer should also be done by HVDC system based on following equation for the d-component of reference current.

$$i_{d-h1}^* = \frac{P_{ref}}{v_d} \tag{14}$$

This equation generates reference current at fundamental frequency. P_{ref} is the active reference power for HVDC system and $v_d$is the d-component of the PCC voltage. According to Fig.4, the reference current for HBCC block is a combination of harmonic currents and fundamental currents as:

$$i_{tot}^* = i_{h1} + i_h^{\sim} \tag{15}$$

In order to have harmonic compensation capability, $i_h^{\sim}$ have to be determined by harmonic injection block. The current which is sampled from the load side should be transformed from abc to αβ reference frame according to the equation (16).

$$\begin{bmatrix} i_\alpha \\ i_\beta \\ 0 \end{bmatrix} = \sqrt{\frac{2}{3}} \begin{bmatrix} 1 & -\frac{1}{2} & -\frac{1}{2} \\ 0 & \frac{\sqrt{3}}{2} & -\frac{\sqrt{3}}{2} \\ \frac{1}{\sqrt{2}} & \frac{1}{\sqrt{2}} & \frac{1}{\sqrt{2}} \end{bmatrix} \begin{bmatrix} i_a \\ i_b \\ i_c \end{bmatrix} \tag{16}$$

As shown in Fig.5.a, this current would be entered into the self-tune filter(STF) which has the capability to extract the desired harmonic frequency and is defined in its predetermined set point frequency[22, 23]. K is the gain coefficient of the STF and is defined based on variation of different values in order to achieve better performance. Fig.5.b shows the bode diagram of STF

block for different values of K. the lower the K, the more precise the extraction of desired component but decreasing K may leads to low response speed of this block.

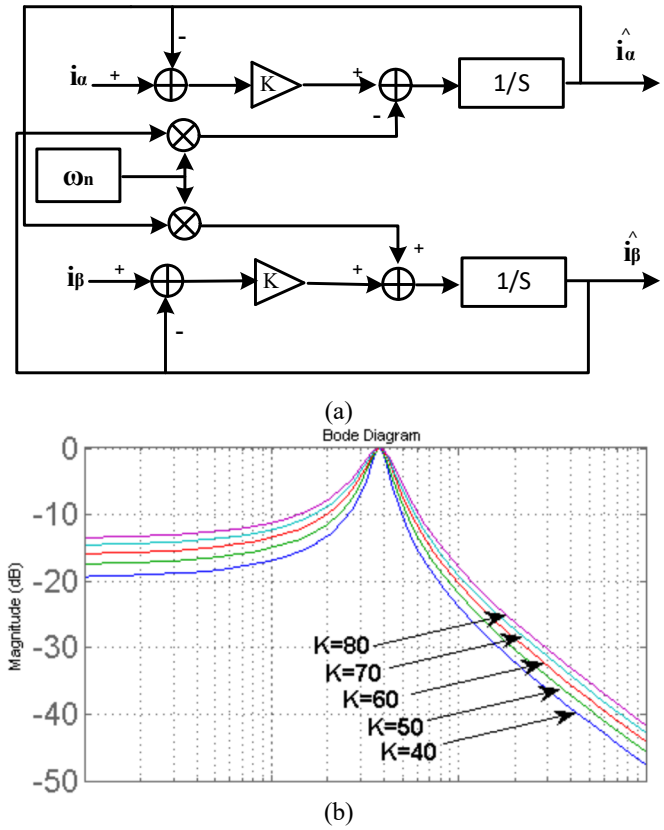

Figure 5. (a) Diagram of the Self-Tune Filter (STF) (b) bode diagram of the STF block for different values of K

$\omega_n$is the set point frequency of the desired harmonics and K is the gain coefficient of the STF which have to be smaller to increase the accuracy of harmonic extraction. By setting the $\omega_n$in the fundamental frequency (50 Hz) and subtracting the output of STF from its input ($\hat{i_{\alpha\beta}}$), remaining harmonics can be achieved. These harmonics have to be injected into the grid by inverter to act as an APF. By inverting these from αβ to abc by equation (17), the reference values of inverter current would be generated in three phase.

$$\begin{bmatrix} i_a \\ i_b \\ i_c \end{bmatrix} = \sqrt{\frac{2}{3}} \begin{bmatrix} 1 & 0 & -\frac{1}{2} \\ -\frac{1}{2} & \frac{\sqrt{3}}{2} & \frac{1}{\sqrt{2}} \\ -\frac{1}{2} & -\frac{\sqrt{3}}{2} & \frac{1}{\sqrt{2}} \end{bmatrix} \begin{bmatrix} i_\alpha \\ i_\beta \\ i_0 \end{bmatrix} \quad (17)$$

By entering these amounts to the hysteresis pulse modulation block and compare them with the actual values, the ideal switching pattern would be generated for correct operation of converter. In an inverter, different switches are turned on and off based on a PWM pattern to generate an AC voltage at the output. Figure 6 shows the main principle of HBCC in which the actual current is compared with reference current. Upper and lower bands are considered around the current. When current passes upper and lower bands, inverter leg switches changes in such a way to bring the current back between band by

changing the leg voltage polarity[24]. Other modified versions of this switching strategy has been analysed in many researches[25, 26].

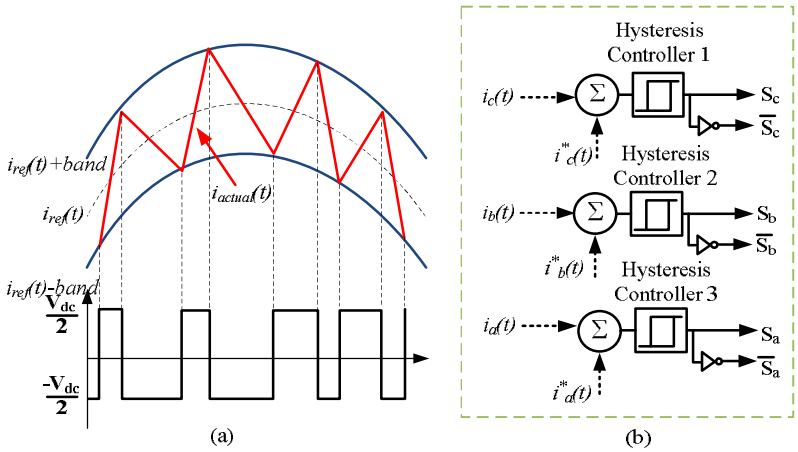

Figure 6.(a) Reference current, upper and lower bands in HBCC and generated voltage (b) HBCC with 3 separated controllers for each converter leg.

3.Case Studies and Results

Table 1 shows simulation parameters for a three terminal MTDC of Fig.1 in which two wind farms are connected to a DC line and the power is transferred to AC grid and an unbalanced nonlinear industrial load. A π model of the line is considered in the simulation. Determination of an HVDC line model (R, C, L) is the same as AC line model with considering a very low frequency (near zero). Line resistance is 0.01 to 0.02 Ω/km, which is the inherent characteristic of the material (in this case 0.015 Ω/km is considered). Conductor inductance is around 1mH/km and its capacitance is 10 nF/km [27- 29]. All simulations are carried out with MATLAB SIMULINK R2013a and the processor for the calculations is Intel(R) Core(TM) i7-4700HQ CPU @ 2.40GHz.

Table 1. Simulation Parameters

Parameters	value
Input voltage source(wind turbine)	3 phase, 600 V, 60 Hz
Wind farm side transformer	Yg/D , 600/240 V
Grid side transformer	D/D , 380/380 V
Transformer Power Rating (VA)	50000
Interfacing resistance (R_c)	0.1mΩ/phase
Interfacing inductance (L_c)	2mH/phase
DC Capacitors (C)	375μF Each side
Line model	75 km model ,π
AC Grid	380 V 50 Hz
Switching/Sampling frequency (f_{sw})	3000 Hz
DC-link voltage set point (V_{dc_ref})	700 V
Grid resistance (R_g)	0.1mΩ Per phase
Grid inductance (L_g)	5 mH Per phase
Voltage source converters(VSC)	2 Level ,3 arm , IGBT/Diode
three phase diode converter load (Nonlinear Load1)	R=30Ω and l= 20mH
single phase diode converter load(Nonlinear Load2)	R=20Ω and l= 20mH

Voltage rating of proposed converters and the transformer are mentioned in Tables 2 and 3, respectively. The parameters are used for the proof of concept.

Table 2. Parameters for wind farm and grid side converters

VSCs parameters	WFSVSC	GSVSC
S_b (VA)	15000	15000
$V_{ph\text{-}ph}$ (V)	240	380
V_{dc} (V)	700	700
I (A)	50	25
C (μF)	375	375

Table 3. Ratings of the transformer

Transformers parameters	Wind farm side	Grid side
P_n(VA)	50000	50000
f_n(Hz)	60	50
Winding 1 parameters	$V_{1\ Ph\text{-}Ph}$ (V_{rms})=600 R_1(pu)=0.04 L_1(pu)=0.04	$V_{1\ Ph\text{-}Ph}$ (V_{rms})=380 R_1(pu)=0.04 L_1(pu)=0.04
Winding 2 parameters	$V_{2\ Ph\text{-}Ph}$ (V_{rms})=240 R_2(pu)=0.04 L_2(pu)=0.0	$V_{2\ Ph\text{-}Ph}$ (V_{rms})=380 R_2(pu)=0.04 L_2(pu)=0.0
Magnetization resistance	R_m (pu)=500	R_m (pu)=500
Magnetization inductance	L_m (pu)=500	L_m (pu)=500

The DC capacitor value can be calculated as [27]:

$$C = \frac{2\tau S_b}{u_{dc,b}^2} \tag{18}$$

Where C is the total capacitance of DC side (μF), τ is DC capacitors time constant (ms), S_b is the nominal Apparent power of the converter (VA), $u_{dc,b}$is the nominal DC voltage (V). τ can be selected between 5-10 ms in order to reduce ripples of DC link and also have a proper system response during power changes. A 375 μF is used in this paper by considering time constant of 6ms.

Two following scenarios are considered for the simulation analysis in this study.

3.1. Control of WFSVSC

At first, variations of the wind farm for both voltage magnitude and frequency are examined. Figure 7 shows reaction of this converter control to the variations of wind farm under four worst case scenarios for frequency and magnitude changes. These scenarios may seem to be unrealistic but performance of the WFSVSC and its control strategy to regulate the voltage under different circumstances can be verified in sever conditions. This means, if the control system can work in this situation,

it will have suitable performance in real conditions of wind turbines operation that are simpler than simulation assumption. As depicted in figures, V_{abc1} and V_{abc2} are the output voltage of wind turbines 1 and 2 respectively. $v_{dc}$is the dc voltage in the output of rectifier and v_{dc-rec} is the dc voltage in the input of inverter after passing from dc line. The objective is to maintain the dc voltage in the 700 V set point voltage level.

The first type of changes is the ramp type (see Fig .7.a), which is the common type of changes in wind farm turbines. In the real circumstances, changes in the variable elements depends on wind speed and power. Changes are applied between $t_1$and t_2 that are shown with dash lines in figures. Results show that for ramp changes of WT_1 and WT_2 voltages in Fig.7.a, the DC link voltage tracks its reference values. Step changes of the voltage (see Fig .7. b) is also simulated which leads to a good performance as well. Another type of variation is the frequency step change by 10 Hz increment (decrement) of WT_1 (WT_2). Figure 7.c shows that the DC link voltage is changed after frequency variations but transients are damped after a short time. A 50 Hz/s ramp frequency variation is also tested, as shown in Figure 7.d. WT_1's frequency is increased by this rate while WT_2's one is decreased by this rate. The control scheme is able to fix the DC link voltage in its predetermined amount.

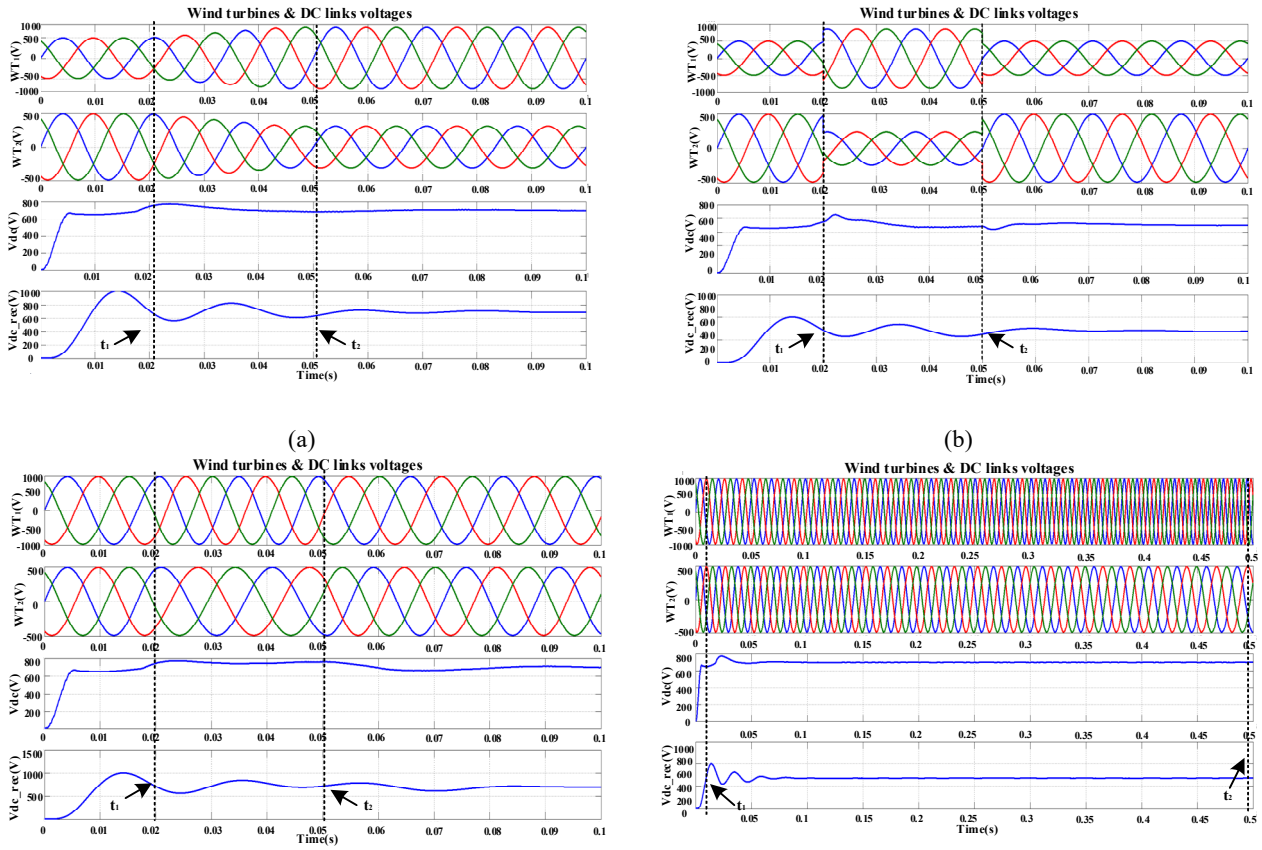

Figure 7.(a) ramp type variation of the wind turbines voltages (b)step type variation (c) step type frequency variation by 10 Hz increment (decrement) for WT_1 (WT_2) (d) ramp type frequency variation by 50 Hz/s increment (and decrement) for WT_1 (WT_2)

3.2. Control of GSVSC

Control scheme of GSVSC should be able to transmit the maximum input power to the grid in different situations. Grid connection on the consumption side is modelled in two forms: HVDC system connected to (1) the stable grid and (2) the grid and an unbalanced nonlinear load at PCC. Figure 8 shows DC link voltages of rectifier output voltage, DC link voltage of inverter input and network current and voltage. The control scheme eases synchronous connection of the HVDC system to the grid with injection of least the amount of the current harmonics (PF=1 and current THD less than 3%).

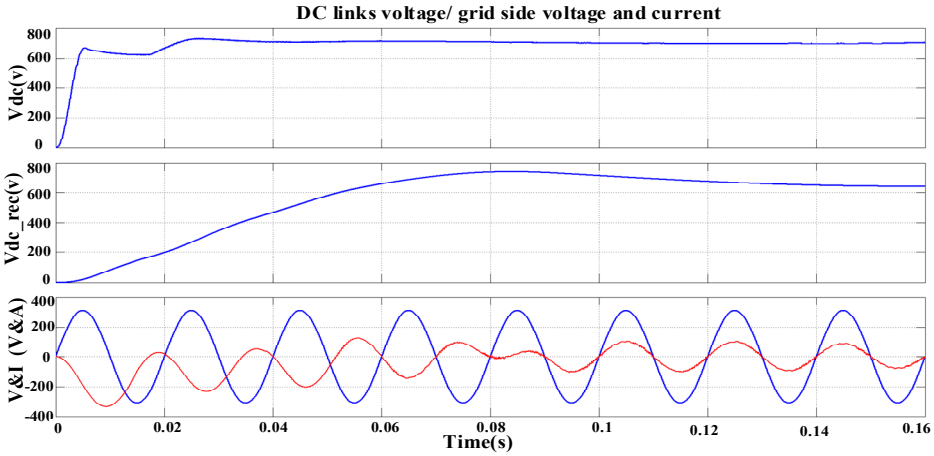

Figure 8. Connection to the stable grid.

As mentioned before, high power nonlinear loads are used in some industrial applications, which draw harmonic contents from grid and distort grid power quality. In this paper, a three phase unbalanced nonlinear load is connected to PCC of grid and HVDC. As shown in Fig.4, a three phase diode rectifier with RL load connected to a single phase rectifier is used to model a load with non-sinusoidal unbalanced currents. In this case, the control scheme of GSVSC should connect the HVDC line to the grid with a power factor correction capability and THD reduction. Figure9 shows HVDC, grid and load current of mentioned system while before HVDC connection (by the breaker shown in Fig.4.), nonlinear load distorts the grid (THD=34%, PF=0.8). When the HVDC system is connected to the network, GSVSC control scheme is able to transmit the maximum power to the grid. The grid voltage and current are in phase with current with a minimum grid current THD (PF=1 and THD=1.9%).

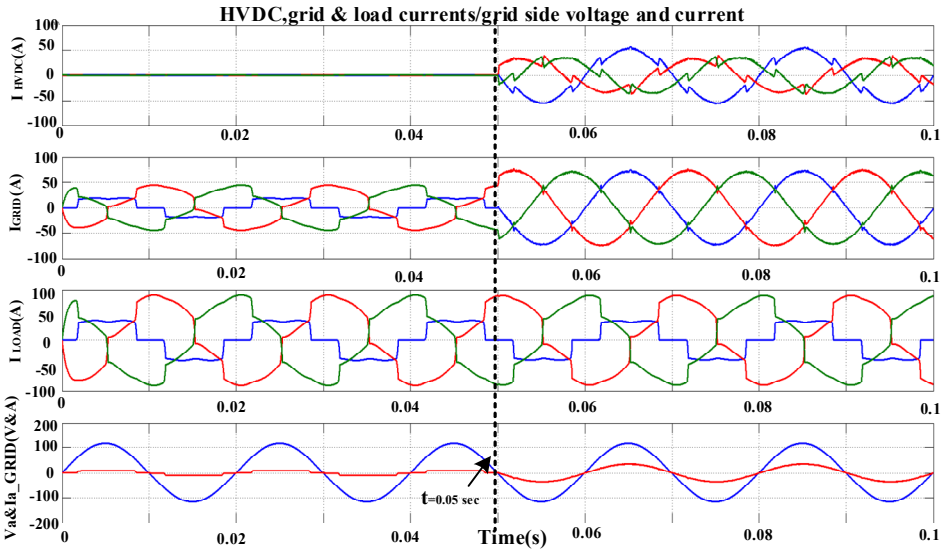

Figure 9. Connection to the grid and unbalanced nonlinear load.

Figure 10 shows the current trajectories of AC grid for more clarifications. Figure 10.a shows the load current from the grid before HVDC connection to the grid in βα frame. After connection of HVDC link, grid current waveform converts to a circle waveform which shows a sinusoidal current (Fig.10.b).

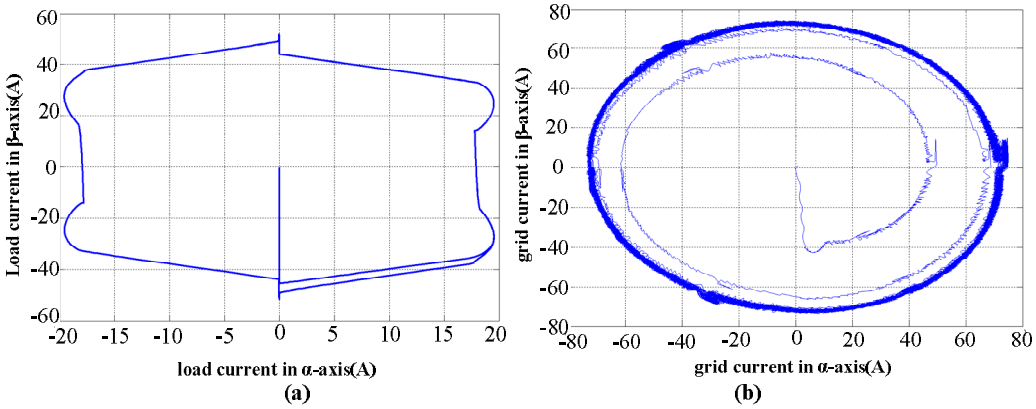

Figure 10. Current trajectories of grid current (a) before HVDC connection (b) after HVDC connection to the PCC.

3.3. A Four-Terminal System

A four-terminal system is considered in order to illustrate the performance of proposed method. This system consists of three wind turbines with different conditions (Ramp changes of generated voltage are tested for the wind turbines connected at terminals 1 and 2 while third turbine is considered with constant output voltage). According to the simulation results of Fig.11, the controller can regulate the DC voltage for a larger network with more generators.

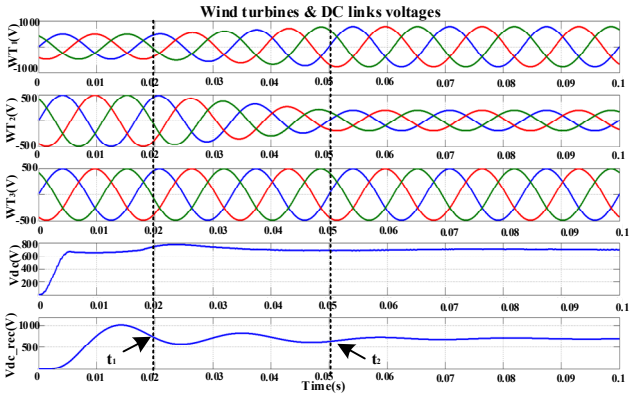

Figure 11. DC voltage regulation for a 4-terminal network with three wind turbines

To scale up the voltage and power, a four terminal system is implemented with realistic data. These data are extracted from Gotland HVDC Light project [31-33], which was among the first implementation of HVDC Light technology. The converter topology and the type of application are pretty close to the analysis of the paper. Table. 4 shows the basic parameters of the mentioned system. Simulations are carried out for the variations of generated voltage at the terminals of WT_1, and WT_2 with a constant voltage of WT_3. The electrical power from the generator is at 60 Hz, AC power with 600V output for large wind turbines. A transformer may be required to increase or decrease the voltage so it is compatible with the end use, distribution or transmission voltage, depending on the type of interconnection. Rectifiers receive 80 kV AC voltage with mentioned variations. Note that the variations are arbitrary and do not reflect a real case, but a very sever condition is considered in the increment or decrement rate of the voltage in order to verify the effectiveness of the proposed control system. DC link voltage at rectifier side and after passing through HVDC line is shown in Fig.12. According to the mentioned results, proposed control strategy can track the reference voltage and control the system in every voltage and power levels.

Table4. Parameters of a 50 MW HVDC Light system

Power rating	50 MW
AC voltage	80 kV(both ends)
DC voltage	80 kV
Length of DC cable	70 km (sub marine cable)
Converters topology	2-level (IGBT series connected)

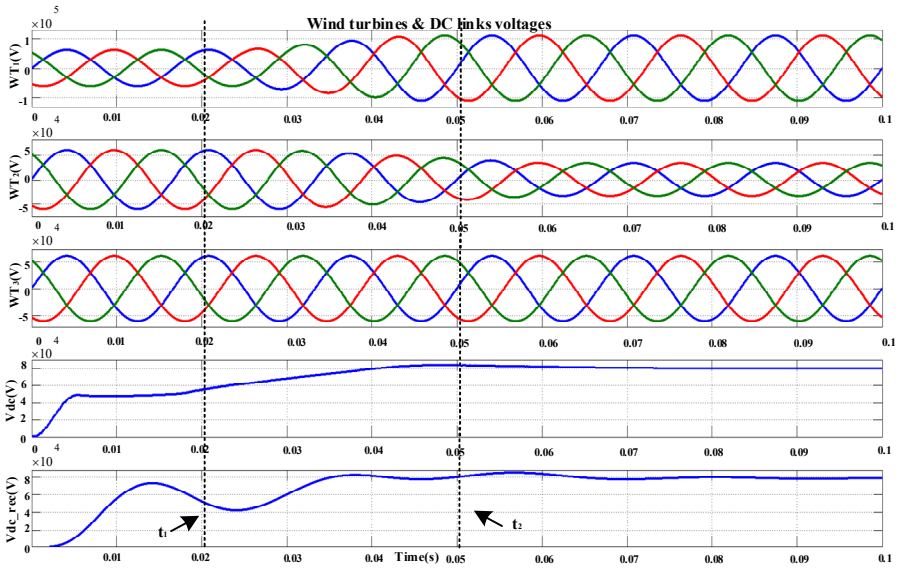

Figure 12. DC voltage regulation for a 4-terminal network 50 MW system

4. Conclusion

This paper presented a novel control strategy for wind farms integrated with the AC grid through a VSC-HVDC link. Due to inherent variations of output voltage in wind turbine generators in terms of amplitude and frequency, the proposed control strategy has the ability to control the converters to provide a DC line with constant voltage. Different types of variation were simulated, thoroughly demonstrating the ability of the control strategy to regulate the voltage. The control strategy was also investigated for the grids connected to high power unbalanced nonlinear loads and the proposed strategy successfully compensated current harmonics and delivered required active and reactive powers to the network. To scale up the voltage and power, a four terminal proposed system was also implemented with realistic data. Again, the proposed control strategy was able to track the reference voltage and control the system in every voltage and power levels.

5. Acknowledgment

This work was supported by FEDER funds through COMPETE 2020 and by Portuguese funds through FCT, under Projects FCOMP-01-0124-FEDER-020282 (Ref. PTDC/EEA-EEL/118519/2010), POCI-01-0145-FEDER-016434, POCI-01-0145-FEDER-006961, UID/EEA/50014/2013, UID/CEC/50021/2013, UID/EMS/00151/2013 and SFRH/BPD/102744/2014. Also, the research leading to these results has received funding from the EU Seventh Framework Programme FP7/2007-2013 under grant agreement no. 309048

6. References

[1] M. Baradar and M. R. Hesamzadeh. A stochastic SOCP optimal power flow with wind power uncertainty. in PES General Meeting| Conference & Exposition, 2014: 1-5.

[2] T. Hammons, D. Woodford, J. Loughtan, M. Chamia, J. Donahoe, D. Povh, et al.Role of HVDC transmission in future energy development. IEEE Power Engineering Review, 2000; 20: 10-25.

[3] M de Prada Gil, O Gomis-Bellmunt, A Sumper, J Bergas-Jané.Power generation efficiency analysis of offshore wind farms connected to a SLPC (single large power converter) operated with variable frequencies considering wake effects.Energy, 2012; 37 (1): 455-468.

[4] W. Lu and B.-T. Ooi. Optimal acquisition and aggregation of offshore wind power by multiterminal voltage-source HVDC. IEEE Transactions on Power Delivery, 2003;18: 201-206.

[5] O. Gomis-Bellmunt, J. Liang, J. Ekanayake, R. King, and N. Jenkins. Topologies of multiterminal HVDC-VSC transmission for large offshore wind farms. Electric Power Systems Research 2011; 81: 271-281.

[6] M. Bahrman and B. Johnson. The ABCs of HVDC transmission technologies. IEEE Power and Energy Magazine, 2007; 2: 32-44.

[7] M De-Prada-Gil, F Díaz-González, O Gomis-Bellmunt, A Sumper.DFIG-based offshore wind power plant connected to a single VSC-HVDC operated at variable frequency: Energy yield assessment. Energy, 2015; 85(15): 311-322.

[8] M de Prada Gil, O Gomis-Bellmunt, A Sumper, J Bergas-Jané.Analysis of a multi turbine offshore wind farm connected to a single large power converter operated with variable frequency. Energy, 2011; 36 (5): 3272-3281.

[9] S.H. Ashrafi Niaki, H. Kazemi Karegar, M. Ghalei Monfared.A novel fault detection method for VSC-HVDC transmission system of offshore wind farm.International Journal of Electrical Power & Energy Systems, 2015; 73: 475-483.

[10] J. Beerten, R. Belmans. A comprehensive modeling framework for dynamic and steady-state analysis of voltage droop control strategies in HVDC grids.International Journal of Electrical Power & Energy Systems, 2015; 73: 691-701.

[11] M. Darabian, A. Jalilvand, M. Azari. Power system stability enhancement in the presence of renewable energy resources and HVDC lines based on predictive control strategy.International Journal of Electrical Power & Energy Systems, 2016; 80: 363-373.

[12] Jie Guo, Daozhuo Jiang, Yuebin Zhou, Pengfei Hu, Zhiyong Lin, Yiqiao Liang. Energy storable VSC-HVDC system based on modular multilevel converter.International Journal of Electrical Power & Energy Systems,2016, 78: 269-276.

[13] Shagufta Khan, Suman Bhowmick.Generalized power flow models for VSC based multi-terminal HVDC systems. International Journal of Electrical Power & Energy Systems, 2016, 82: 67-75.

[14] J. Reeve and M. Sultan. Gain scheduling adaptive control strategies for HVDC systems to accommodate large disturbances. IEEE Transactions onPower Systems1994; 9: 366-372.

[15] L. Pilotto, M. Roitman, and J. Alves. Digital control of HVDC converters. IEEE Transactions on Power Systems, 1989; 4: 704-711.

[16] J. D. Ainsworth. The phase-locked oscillator-a new control system for controlled static convertors. IEEE Transactions on Power Apparatus and Systems, 1968: 859-865.

[17] J. Liang, O. Gomis-Bellmunt, J. Ekanayake, N. Jenkins, and W. An. A multi-terminal HVDC transmission system for offshore wind farms with induction generators. International Journal of Electrical Power & Energy Systems, 2012; 43: 54-62.

[18] D. Povh, P. Thepparat, and D. Westermann. Further development of HVDC control. in PowerTech: 1-8.

[19] F. Karlecik-Maier. A new closed loop control method for HVDC transmission. IEEE transactions on power delivery, 1996; 11: 1955-1960.

[20] T. Haileselassie, K. Uhlen, and T. Undeland. Control of multiterminal HVDC transmission for offshore wind energy. in Nordic Wind Power Conference, 2009, pp. 10-11

[21] C. Ismunandar, A. A. van der Meer, M. Gibescu, R. L. Hendriks, and W. L. Kling. Control of multi-terminal VSC-HVDC for wind power integration using the Voltage-Margin method. in Proc. 9th Int. Workshop on Large-Scale Integration of Wind Power Into Power Systems as Well as on Transmission Networks for Offshore Power Plants, 2010, pp. 18-19

[22] H. Akagi. Active and hybrid filters for power conditioning. ISIE, 2000: 26-36.

[23] M Mehrasa, E Pouresmaeil, MF Akorede, BN Jørgensen, JPS Catalão.Multilevel converter control approach of active power filter for harmonics elimination in electric grids.Energy, 2015; 84: 722-731

[24] E. Pouresmaeil, M. F. Akorede, D. Montesinos-Miracle, O. Gomis-Bellmunt, and J. C. T. Caballero. Hysteresis current control technique of VSI for compensation of grid-connected unbalanced loads. Electrical Engineering, 2014; 96: 27-35.

[25] E. Pouresmaeil, M. Mehrasa, and J. P. Catalao. A Multifunction Control Strategy for the Stable Operation of DG Units in Smart Grids.IEEE Transactions on Smart Grid,2015; 6: 598-607.

[26] E. Pouresmaeil, C. Miguel-Espinar, M. Massot-Campos, D. Montesinos-Miracle, and O. Gomis-Bellmunt. A control technique for integration of DG units to the electrical networks. IEEE Transactions on Industrial Electronics, 2013; 60: 2881-2893.

[27] Chuiqing Du. VSC-HVDC for Industrial Power Systems. Ph.D. dissertation, Energy and Environment Dept., Chalmers University of Technology, Goteborg, Sweden, 2007.

[28] M .Szechtman T. Wess C .V Thio.A Benchmark Model for HDC System Studies. CEPEL, Brazil FGH, Germany Manitoba Hydro, Canada.

[29] Paulo Fischer de Toledo. Modelling and control of a line-commutatedHVDC transmission system interactingwith a VSC STATCOM. TRITA-EE-2007-040ISSN 1650-674X.

[30] Yuriy Kazachkov Jay Senthil . HVDC Modeling Experience in PSSE. SIEMENS Energy Inc.2011.

[31] N. Flourentzou, V. G. Agelidis, and G. D. Demetriades. VSC-based HVDC power transmission systems: An overview.IEEE Transactions on Power Electronics, vol. 24, pp. 592-602, 2009.

[32] ABB library and references for HVDC: www.abb.com/hvdc.

[33] U. Axelsson, A. Holm, C. Liljegren, M. Aberg, K. Eriksson, and O .Tollerz. The Gotland HVDC Light project-experiences from trial and commercial operation. in Electricity Distribution, 2001. Part 1: Contributions. CIRED. 16th International Conference and Exhibition on (IEE Conf. Publ No. 482), vol. 1, 2001.